

The Effects of an Electromagnetic Crystal Substrate on a Microstrip Patch Antenna

Kamil Agi, *Member, IEEE*, Mohammad Mojahedi, *Member, IEEE*, Babar Minhas, *Student Member, IEEE*, Edl Schamiloglu, *Fellow, IEEE*, and Kevin J. Malloy, *Member, IEEE*

Abstract—The effects of a two-dimensional (2-D) electromagnetic bandgap substrate on the performance of a microstrip patch antenna are investigated. The microstrip patch antenna is placed on a defect in the electromagnetic bandgap substrate that localizes the energy under the antenna. Finite-difference time-domain calculations are employed to determine the effects of the substrate. The excitation frequency of the antenna near the resonance frequency of the defect mode can be used to control the coupling between antennas that are placed in an array.

Index Terms—Electromagnetic bandgap materials, integration, microstrip patch antennas.

I. INTRODUCTION

ELECTROMAGNETIC bandgap materials (EBMs) are a new class of periodic metallic, dielectric, or composite structures that exhibit transmission (pass) and reflection (stop) bands in their frequency response [1]. Also known as photonic crystals, the bands in the EBMs occur due to the constructive and destructive interference of the electromagnetic waves within the crystal. When the stopbands exist for waves in all directions, the band is called “forbidden gap,” and the EBMs are sometimes referred to as photonic band gap materials. If the periodicity in an EBM is perturbed by either removing or adding a material with a different dielectric constant, size, or shape, a “defect” state is created in the forbidden gap, where an electromagnetic mode is allowed, and localization of the energy occurs [1].

Because of the properties described above, EBMs are currently being used in many novel microwave applications. For example, they are used as filters in microstrip lines [2], [3], as high-power microwave components [4], and as substrates for printed antenna structures [5]–[9]. Theoretical descriptions of EBMs thus far have been limited to the plane wave expansion method for infinitely long and uniform crystal [10]–[12], scattering matrix method [13]–[15], transfer matrix method [16],

and finite-difference time-domain (FDTD) analysis of a photonic crystal waveguide [17]. Since, in many applications, EBM has finite size of a few lattice constant or is accompanied by a finite ground plane, from all the above approaches, the FDTD seems to be more advantageous [18], [19]. This becomes more evident when one has to study the combined behavior of an antenna with an EBM substrate.

For the antenna applications of EBMs, much of the earlier work has been based on integrating *simple* antenna structures (dipoles, bowties, etc.) with three-dimensional (3-D) EBMs [6]–[9], [20]. The basic idea is that since an antenna placed on a dielectric substrate radiates more efficiently into the dielectric substrate than the air side¹ [21], one must replace the substrate with an EBM whose forbidden gap encompasses the antenna excitation frequency. In this manner, provided there are no surface modes, the power previously radiated into the substrate will be reflected toward the air side.

Although the above approach has led to somewhat more efficient antennas, the measured antenna responses are not enhancement as originally expected [20]. This is partly because the dispersion in the EBM substrate complicates the simple *design equations*, and one must take into account both the magnitude and phase of the waves reflected from the EBM substrate, partly because the multiple reflection from the substrate and its interaction with the radiated field must be accounted for. To make the matters more complicated, the location of the feed point of the antenna is also a critical parameter in obtaining a *reasonable* antenna pattern. It is clear, therefore, that manufacturing an efficient antenna with an EBM substrate is a challenge.

To simplify the work, there are few steps that may be considered. For example, to use the simple *design equations*, one may characterize the EBM substrate in terms of an effective (or equivalent) index of refraction [22], with both real and imaginary parts, to take into account both the magnitude and the phase of the reflected waves. Another attempt may be to replace the 3-D EBM substrate used in [6]–[9] and [20] with a *simpler* 2-D electromagnetic bandgap material (2-DEBM) substrate [23]–[25]. This is of particular interest in the case of microstrip patch antennas (MPAs) since eliminating the radiation into the substrate (the energy trapped between the two metallic plates) is of no immediate concern, whereas inhibiting the propagation of the surface modes is. Finally, an FDTD method can be used to take into account the multiple reflection, in addition to gaining insight to the problem of electromagnetic wave interactions with the substrate.

¹For a slot antenna and an elementary dipole, the power radiated into the substrate is proportional to $\epsilon_r^{3/2}$ and $\epsilon_r^{1/2}$, respectively, where ϵ_r is the substrate dielectric constant.

Manuscript received April 15, 2001; revised April 15, 2002. This work was supported in part by the U.S. Army Research Office under Grant DAAH04-96-1-0439.

K. Agi is with K&A Wireless, LLC, Albuquerque, NM 87112 USA (e-mail: kagi@ka-wireless.com).

M. Mojahedi is with the Department of Electrical and Computer Engineering, University of Toronto, Toronto, ON M5S 3G4 Canada (e-mail: mojahedi@waves.utoronto.ca).

B. Minhas and K. J. Malloy are with the Center for High Technology Materials, Electrical and Computer Engineering Department, University of New Mexico, Albuquerque, NM 87111 USA.

E. Schamiloglu is with the Pulsed Power Laboratory, Electrical and Computer Engineering Department, University of New Mexico, Albuquerque, NM 87111 USA (e-mail: edl@ecece.unm.edu).

Publisher Item Identifier S 0018-926X(02)04960-8.

MPAs are known for their many desirable physical characteristics such as, low profile, low cost, light weight, easy fabrication, and conformability. They have found applications in communication systems, as well as many other systems that require compact antenna structures [26]. The conventional microstrip antenna is a metallic patch of an arbitrary shape that is placed a certain distance, typically less than 0.01λ , where λ is the wavelength of the electromagnetic radiation, above a metallic ground plane. They are typically excited using a coaxial probe through the ground plane, as shown in Fig. 1(a), or by a microstrip line in the plane of the antenna [26].

Because of its resonance nature, the MPA has inherently a narrow bandwidth, limiting its wide spread application. However, there are some techniques that may be used to increase the bandwidth [26]–[30], but they all invariably increase the antenna volume by either increasing the patch size or the substrate thickness. This approach, while in principle can produce bandwidths as high as 20% [27], greatly reduces the antennas efficiency due to the increased surface wave losses [26]–[31]. In other words, the increase in the substrate thickness causes the antenna to more efficiently excite the substrate and surface modes, which in turn removes energy from the main radiation lobe.

To understand the mechanism responsible for the surface waves generation, a ray optics description can be useful. Considering the MPA shown in Fig. 1(a), the rays within the substrate that are incident on the substrate–air interface with angles greater than the critical angle are internally reflected and are trapped as surface waves [21]. These surface waves may show up as spikes in the antenna pattern [21], [32] and can dominate the radiated power.

EBM substrate is a simple solution to the problem of surface waves. If an EBM is designed such that the frequencies of the substrate modes fall within the stopband, the excited substrate modes will exponentially decay, hence reducing the energy lost into the substrate and increasing the energy coupled to the radiated field. Yang *et al.* originally proposed that high-gain antenna structures could be obtained by printing an antenna on a 2-DEBM [24]. In this work, 2-DEBMs are employed as a means of eliminating the substrate and surface modes for patch antennas. In addition, a 2-DEBM antenna structure is fabricated with a defect point in the EBM substrate placed under the patch location. This point defect is used to localize the field within the defect region, hence confining the energy under the patch. The energy confinement leads to a more efficient antenna as well as providing a simpler method of fabrication.

The remainder of the paper is organized as follows. Section II will provide a brief description of the FDTD method and the commercial package used for its implementation. Section III is a description of the experimental setup used to validate the code. Section IV determines the response of the EBM substrate with and without the point defect and the 2-DEBM antenna structure. Section V presents the conclusions.

II. FDTD METHOD

The FDTD code used in this work is XFDTD® (Version 4.06), which is a commercial code available through Remcom,

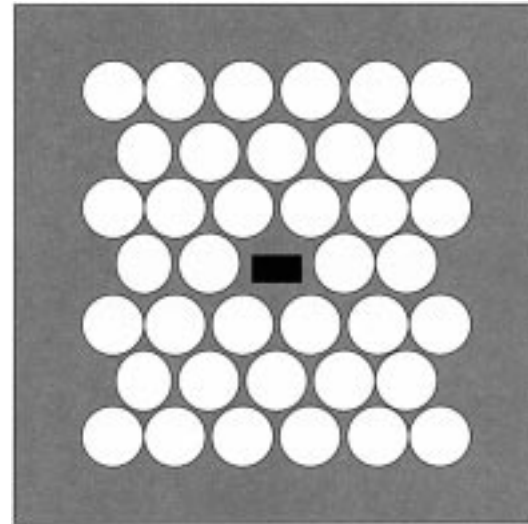
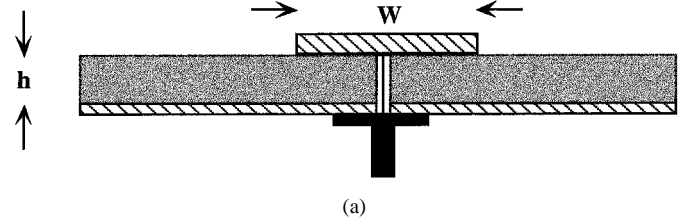


Fig. 1. (a) Conventional patch antenna using a coaxial probe excitation. (b) 2-D electromagnetic bandgap substrate that is integrated with a conventional patch.

Inc.² The code is based on the standard Yee cell geometry, and the values of the electric and magnetic fields are calculated in consecutive time steps [18]. The utility of the approach is its ability to calculate S-parameters [18], [33]. In addition, steady-state field plots are obtained to provide physical insight into the problem and the effects of the EBM substrate. The two antennas compared in this work are shown in Fig. 1(a) and (b). Two sets of simulations are performed. The initial set of simulations is used to validate the code through experimental verification. The second set of simulations is used to compare a conventional patch antenna (without EBM substrate) with one that is integrated with a 2-DEBM. The effects of the EBM substrate with and without the defect is also investigated.

For the initial set of simulations, the patch has a width of 8 mm in the x -direction and a length of 4.14 mm in the y -direction. A Cartesian coordinate system is employed, and the antenna geometry is broken up into a grid of $\Delta x = 0.4$ mm, $\Delta y = 0.414$ mm, and $\Delta z = 0.25$ mm in a space of $75 \times 50 \times 25$ cells. The width of the antenna is $20\Delta x$ cells, and the length of the antenna is $10\Delta y$ cells. The substrate in the FDTD calculation is 1.25 mm thick (thereby occupying five cells in the z -direction), with a dielectric constant of 10.2. The antenna is excited on center in the x direction and off center in the y direction at a point 1.656 mm from the bottom edge of the antenna. The time step is taken to be 0.6294 ps, which is set to the Courant limit for a general 3-D grid [18]. The ground plane is assumed to be infinite in extent. All other boundaries are set to be absorbing (Liao-type).

²XFDTD is a registered trademark of Remcom, Inc., University Park, PA, 1998.

For the second set of simulations, the size of the FDTD space is increased such that the effects of the 2-DEBM can be studied. The patch has a width of 8 mm in the x direction and a length of 4 mm in the y direction. The antenna geometry is broken up into a grid of $\Delta x = 0.1$ mm, $\Delta y = 0.1$ mm, and $\Delta z = 0.4233$ mm in a space of $120 \times 135 \times 35$ cells. The substrate in the FDTD calculations is 1.27 mm thick, thereby occupying three cells in the z direction, and has a dielectric constant of 10.2. The time step is taken to be 1.211 ps, which is again set to the Courant limit for a general 3-D grid. The antenna is suspended in the FDTD space ten cells above an absorbing boundary in order to preserve the finite-size effects, and a finite PEC layer is used as a ground plane. All remaining boundary conditions are set to be absorbing (Liao-type).

The antenna is excited with a Gaussian pulse with a width of 121 ps. The coaxial probe excitation of the antenna is shown on Fig. 1(a). It was found that a thin wire was the best type of excitation suited for obtaining reasonable agreement with the experimental results. For the initial set of simulations, the code was run for 10 000 time steps that took approximately 30 min on a Pentium Pro, 300-MHz machine with 256 MB of RAM. For the second set of simulations, the code ran for approximately 5–8 h on the same machine.

III. EXPERIMENTAL SETUP

Two antennas were built for measurement. They both had dimensions consistent with the simulations and were fabricated on a RT-Duroid 6010 substrate with a dielectric constant of 10.2. The thickness of both substrates was 1.27 mm. The first antenna had a uniform dielectric substrate as shown in Fig. 1(a), and the second antenna had the 2-DEBM integrated, which was obtained by drilling holes into the substrate as shown in Fig. 1(b). The EBM substrate had a triangular lattice with lattice constant of 1.38 cm and a hole diameter of 1.27 cm and was originally designed to have a gap at approximately 9 GHz [1]. This gap design is based on an EBM that is infinite in extent in the transverse direction. The antennas return loss (S_{11}) is measured using an HP8510 vector network analyzer.

The network analyzer measurements are compared to the FDTD calculation for the conventional patch antenna. In Fig. 2, the solid line is S_{11} measured using the network analyzer, and the line with the markers is the calculated results using XFDTD[®]. The calculated results are based on the first set of simulations and are in agreement with the experiment. Antenna pattern measurements and discussions of finite ground-plane effects were investigated using these antennas and can be found in [23].

IV. EFFECTS OF THE EBM SUBSTRATE

We have chosen to study the effects of the EBM substrate by computing the transmission coefficient (S_{21}) of a microstrip line on the substrate using XFDTD[®]. In other words, the microstrips shown in Fig. 3 are excited at one end by a Gaussian pulse, and the transmitted pulse is detected at the other end. Since the fields in a microstrip line are confined in the dielectric between the line and the ground plane [34], this scheme is ideal to sample

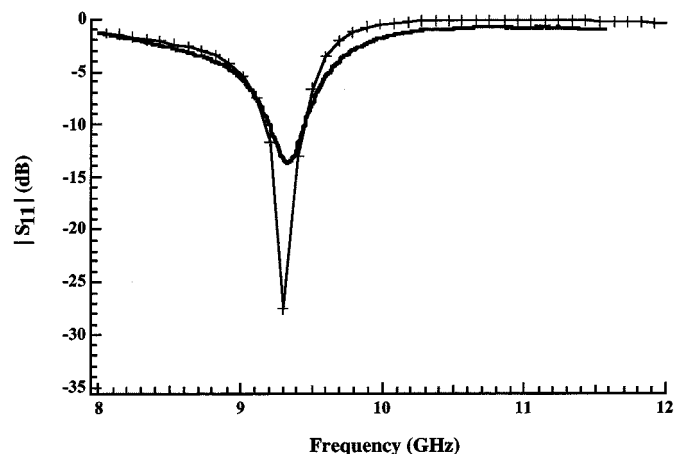


Fig. 2. $|S_{11}|$ measured (solid line) using a network analyzer and calculated (line with markers) using FDTD. There is a good agreement between the calculation and the experiment.

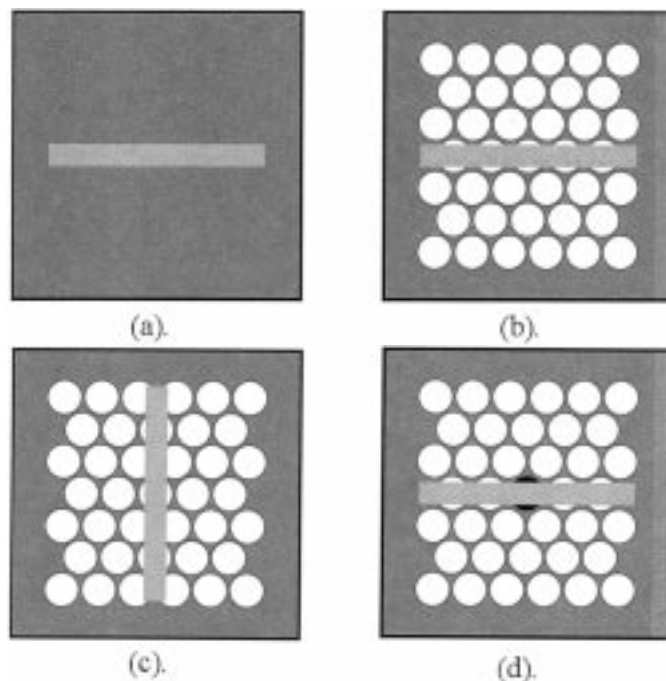


Fig. 3. (a) Horizontally oriented microstrip line on a uniform substrate. (b) Horizontally oriented microstrip line on a 2-DEBM substrate. (c) Vertically oriented microstrip line on a 2-DEBM substrate. (d) Horizontally oriented microstrip line on a 2-DEBM substrate with a defect.

the EBM substrate periodicity. The top views of the structures under investigation are shown in Fig. 3. Fig. 3(a) is a horizontally placed microstrip line on a uniform substrate. Fig. 3(b) and (c) are the horizontally and vertically oriented microstrip lines on a 2-DEBM substrate. Fig. 3(d) is a horizontally oriented microstrip line on a 2-DEBM substrate with a point defect. The microstrip lines investigated all have a width of 4 mm in the x direction and a length of 80 cells. The geometry is broken up into a grid of $\Delta x = 0.1$ mm, $\Delta y = 0.1$ mm, and $\Delta z = 0.4233$ mm in a space of $120 \times 135 \times 35$ cells. The substrate in the FDTD calculations is 1.27 mm thick, thereby occupying three cells in the z direction, and has a dielectric constant of 10.2. The time step is taken to be 1.211 ps.

The frequency range of the stopband can be determined by the computed S_{21} . Fig. 4 shows the calculated S_{21} of a microstrip line on a uniform substrate and the calculated S_{21} of a microstrip line on a 2-DEBM, as indicated. Note that in the case of the 2-DEBM substrate, there is a stopband from 5.5 to 10.5 GHz. This stopband is due to the destructive interference that occurs in the substrate because of the periodic placement of the holes. Using the results presented in [1], for an infinite 2-D structure, the EBM was designed to have a stopband centered at 9 GHz. However, the FDTD results show that the stopband frequency has been reduced for a finite microstrip structure with a ground plane.

The width and location of the stopband depends on the orientation of the microstrip line. Fig. 5 shows the stopbands as a function of the orientation of the microstrip line for two symmetry points. In Fig. 5, the horizontal orientation of the microstrip line is shown as the solid line, and the vertical orientation is shown as the dashed line. The stopband for the horizontally oriented line extends from 5.5 to 10.5 GHz. For the vertically oriented microstrip line, the stopband extends from 5.5 to 10 GHz. Note that for an EBM substrate with triangular unit cell, there is a three-fold rotational symmetry. Therefore, for our geometry, a vertical microstrip line is equivalent to a line rotated 30° away from one of the triangle sides. By overlapping the transmission responses of the horizontally and vertically placed lines, one can obtain the dispersion curve as well as determine the location of the "forbidden gap." Returning to the point expressed in the introduction, in order to increase the antenna efficiency by suppressing the surface modes, one must try to excite the MPA at frequencies within the "forbidden gap."

It is well known that introducing a lattice imperfection, which is also known as defect, can produce a localized modes within the "forbidden gap" [1], [35]. To investigate the effects of a point defect, the same microstrip line as in the previous cases is used, but now, the center hole is filled with a material other than air with dielectric constant of 5.6. The result is shown in Fig. 6, where S_{21} for the microstrip line printed on a 2-DEBM with a point defect (dashed line) and without the defect (solid line) is displayed. The point defect creates a peak in the density of states within the "forbidden gap," where previously, no states were allowed, which is shown as a transmission peak depicted in Fig. 6. Because of the finite size of the crystal, the defect state has a finite bandwidth [35]; however, its location in frequency or its bandwidth can be tuned by varying the dielectric constant or the size of the defect. Fig. 7 is the response of a microstrip line with a defect with dielectric constant of 10.6 (same as the host). In this case, there are two transmission peaks. For the horizontally oriented microstrip line, the first peak is at 6.8 GHz, and the second is at 9.5 GHz. For the vertically oriented microstrip line, the transmission peaks occur at slightly lower frequencies of 6.4 GHz and at 8.5 GHz. For reference, the arrow indicates the excitation frequency and the resonance of the patch antenna. The nature of the defect modes and their resonance frequencies as a function of direction is currently under investigation. Since defect modes can be used to localize the energy at a point, it is expected that they play a critical role in designing a more efficient MPA.

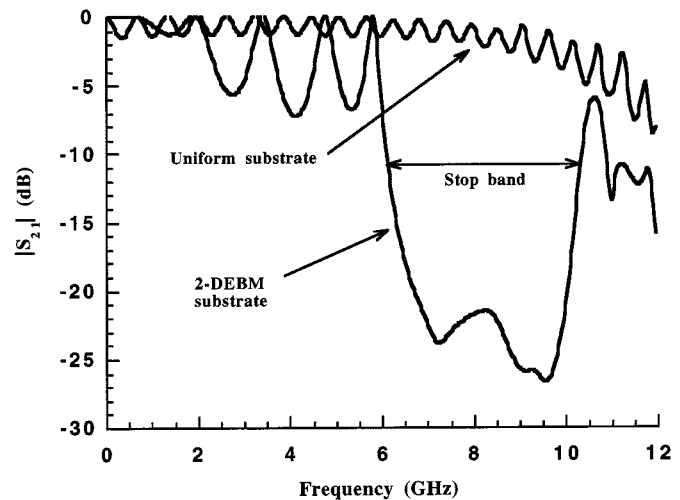


Fig. 4. $|S_{21}|$ for a standard microstrip line on a uniform substrate and a microstrip line placed on a 2-DEBM substrate. Note that the stopband extends from 5.5 to 10.5 GHz.

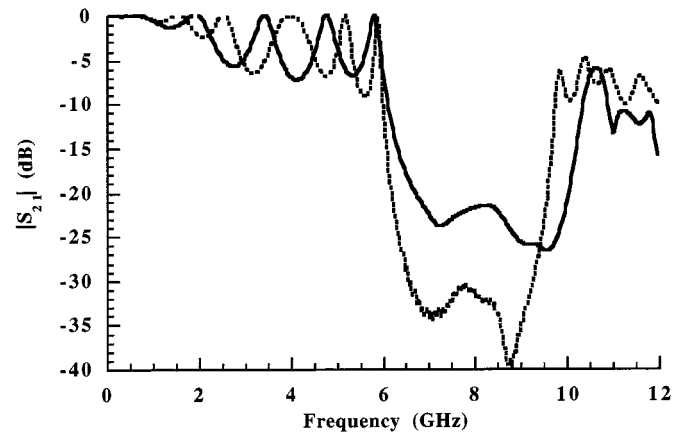


Fig. 5. Magnitude of the S_{21} for a microstrip line placed in the horizontal direction (solid line) and the vertical direction (dashed line). The stopband shifts to lower frequencies for microstrip with the vertical orientation.

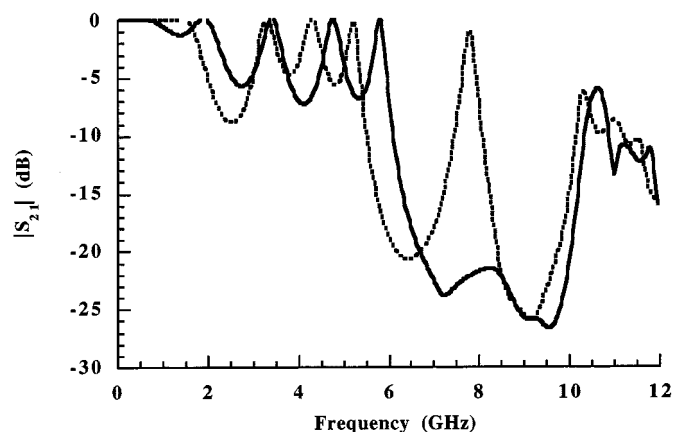


Fig. 6. Magnitude of S_{21} for a microstrip line printed on a 2-DEBM substrate (solid line) and a 2-DEBM substrate with a defect (dashed line). The transmission peak at 7.75 GHz is the result of the defect state.

The motivation behind combining the EBM substrate having a defect with a MPA is as follows. As previously mentioned,

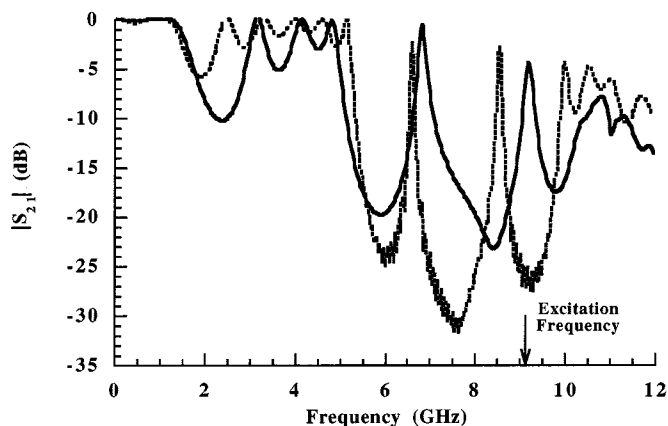


Fig. 7. $|S_{21}|$ for the microstrip line with a defect in the periodicity. The transmission peaks in the stopband are the defect modes. The solid line is the horizontally placed microstrip line, and the dashed line is the vertically placed line. The arrow indicates the excitation frequency of MPA.

in order to suppress the surface modes, one must try to excite the antenna at frequencies within the “forbidden gap.” At the same time, the presence of a point defect immediately under the patch, as shown in Fig. 1(b), allows a higher concentration of the electromagnetic energy density within the cavity formed by the patch and the ground plane, which in turn can increase the radiated energy of the antenna. To make this point more clear, consider Fig. 8, which is a plot of the electric field magnitude (and hence electric energy) in gray scale for the MPA in the vicinity of the defect point. Note that since electric field is largest along the nodal planes of the magnetic field [1], the above intensity plot is a rough estimate of the total energy density. The antenna excitation and the forward scattering coefficient (S_{21}) for the 2-DEBM substrate were shown in Fig. 7. From Fig. 7, it is easy to see that the antenna excitation is tuned to the “horizontal resonance” and away from the “vertical resonance.” In other words, we expect that the energy density will be well confined in the horizontal direction and not so completely confined in the vertical direction. It has previously been shown that for a localized state in the middle of the “forbidden gap,” the electric and magnetic fields are tightly bounded to the defect with a decaying length in the order of one lattice constant [35]–[37]. This length is expected to increase as the localized state moves from the mid-gap toward the continuum. Fig. 8 shows that this seems to be the case for the MPA when the excitation frequency is tuned to the “horizontal defect.” On the other hand, since the excitation frequency is away from the “vertical resonance” and yet within the stopband of the 2-DEBM, one expects that the field along the vertical direction also decays exponentially; however, it has a longer decaying length. This is similar to the leakage of the modes in a Fabry–Perot that has been predicted for a 2-DEBM [15].

Finally, the fact that the antenna leakage can simply be controlled by tuning to or away from a defect resonance line can be used to inhibit or stimulate the coupling between different elements of an MPA array. Therefore, incorporating point defects in a 2-DEBM substrate for MPA also presents itself as a viable approach in designing more efficient antenna arrays.

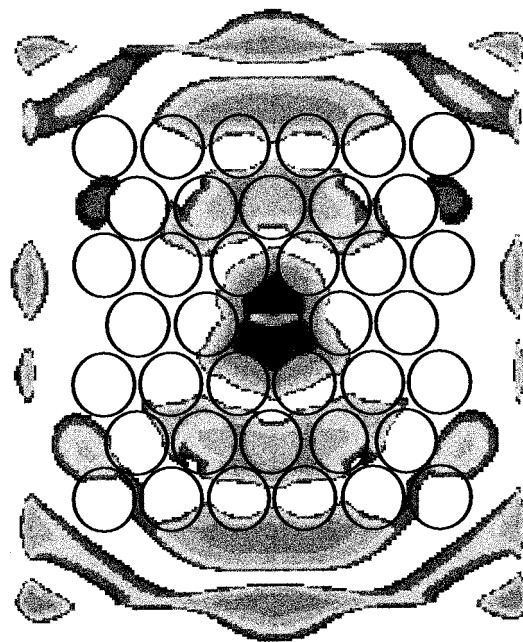


Fig. 8. Electric field intensity plot for a patch antenna on a 2-DEBM substrate with a defect, as determined by FDTD calculations. The antenna excitation is shown in Fig. 7, which results in coupling in the vertical direction.

V. CONCLUSION

A 2-DEBM was integrated with a conventional rectangular MPA. The properties of this structure and the effects of the substrate were studied using a FDTD code. The initial calculations to verify the code compared favorably with the experiment.

The properties of a 2-DEBM substrate were investigated using a microstrip line. The fields of a conventional microstrip line are confined between the line and the ground plane, hence providing an ideal way of sampling the structure. An EBM substrate was designed with a point defect under the antenna site. The presence of the defect can increase the radiated power due to the energy storage under the antenna.

Finally, conventional design tools for MPA are insufficient to determine the optimal coupling into the antenna. A design tool is currently being developed to optimize the incorporation of the antenna with the 2-DEBM having a point defect.

REFERENCES

- [1] J. D. Joannopoulos, R. D. Meade, and J. N. Winn, *Photonic Crystals: Molding the Flow of Light*. Princeton, NJ: Princeton Univ. Press, 1995.
- [2] V. Radisic, Y. X. Qian, R. Coccioli, and T. Itoh, “Novel 2-D photonic bandgap structure for microstrip lines,” *IEEE Microwave Guided Wave Lett.*, vol. 8, pp. 69–71, Jan. 1998.
- [3] I. Rumsey, M. PiketMay, and P. K. Kelly, “Photonic bandgap structures used as filters in microstrip circuits,” *IEEE Microwave Guided Wave Lett.*, vol. 8, pp. 336–338, 1998.
- [4] K. Agi, L. D. Moreland, E. Schamiloglu, M. Mojahedi, K. J. Malloy, and E. R. Brown, “Photonic crystals: A new quasioptical component for high-power microwaves,” *IEEE Trans. Plasma Sci.*, vol. 24, pp. 1067–1071, 1996.
- [5] E. R. Brown, C. D. Parker, and E. Yablonovitch, “Radiation properties of a planar antenna on a photonic-crystal substrate,” *J. Opt. Soc. Amer. B*, vol. 10, pp. 404–407, 1993.
- [6] E. R. Brown and O. B. McMahon, “High zenithal directivity from a dipole antenna on a photonic crystal,” *Appl. Phys. Lett.*, vol. 68, pp. 1300–1302, 1996.

- [7] S. D. Cheng, R. Biswas, E. Ozbay, S. McCalmont, G. Tuttle, and K. M. Ho, "Optimized dipole antennas on photonic band-gap crystals," *Appl. Phys. Lett.*, vol. 67, pp. 3399–3401, 1995.
- [8] M. P. Kesler, J. G. Maloney, B. L. Shirley, and G. S. Smith, "Antenna design with the use of photonic band-gap materials as all-dielectric planar reflectors," *Microwave Opt. Techn. Lett.*, vol. 11, pp. 169–174, 1996.
- [9] M. M. Sigalas, R. Biswas, Q. Li, D. Crouch, W. Leung, R. Jacobs-Woodbury, B. Lough, S. Nielsen, S. McCalmont, G. Tuttle, and K. M. Ho, "Dipole antennas on photonic band-gap crystals: Experiment and simulation," *Microwave Opt. Techn. Lett.*, vol. 15, pp. 153–158, 1997.
- [10] K. M. Leung and Y. F. Liu, "Full vector wave calculation of photonic band structures in face-centered-cubic dielectric media," *Phys. Rev. Lett.*, vol. 65, pp. 2646–2649, 1990.
- [11] Z. Zhang and S. Satpathy, "Electromagnetic-wave propagation in periodic structures: Bloch wave solution of Maxwell equations," *Phys. Rev. Lett.*, vol. 65, pp. 2650–2653, 1990.
- [12] K. M. Ho, C. T. Chan, and C. M. Soukoulis, "Existence of a photonic gap in periodic dielectric structures," *Phys. Rev. Lett.*, vol. 65, pp. 3152–3155, 1990.
- [13] D. Felbacq, G. Tayeb, and D. Maystre, "Scattering by a random set of parallel cylinders," *J. Opt. Soc. Amer. A*, vol. 11, pp. 2526–2538, 1994.
- [14] G. Tayeb and D. Maystre, "Rigorous theoretical study of finite-size two-dimensional photonic crystals doped by microcavities," *J. Opt. Soc. Amer. A*, vol. 14, pp. 3323–3332, 1997.
- [15] J. Yonekura, M. Ikeda, and T. Baba, "Analysis of finite 2-D photonic crystals of columns and lightwave devices using the scattering matrix method," *J. Lightwave Technol.*, vol. 17, pp. 1500–1508, 1999.
- [16] J. B. Pendry and A. Mackinnon, "Calculation of photon dispersion-relations," *Phys. Rev. Lett.*, vol. 69, pp. 2772–2775, 1992.
- [17] A. Mekis, J. C. Chen, I. Kurland, S. H. Fan, P. R. Villeneuve, and J. D. Joannopoulos, "High transmission through sharp bends in photonic crystal waveguides," *Phys. Rev. Lett.*, vol. 77, pp. 3787–3790, 1996.
- [18] K. S. Kunz and R. J. Luebbers, *The Finite Difference Time Domain Method for Electromagnetics*. Boca Raton, FL: CRC, 1993.
- [19] A. Taflov, *Computational Electrodynamics: The Finite-Difference Time-Domain Method*. Boston, MA: Artech House, 1995.
- [20] W. Y. Leung, R. Biswas, S. D. Cheng, M. M. Sigalas, J. S. McCalmont, G. Tuttle, and K. M. Ho, "Slot antennas on photonic band gap crystals," *IEEE Trans. Antennas Propagat.*, vol. 45, pp. 1569–1570, Aug. 1997.
- [21] D. B. Rutledge, D. P. Neikirk, and D. P. Kasilingam, "Integrated-circuit antennas," in *Infrared and Millimeter Waves: Millimeter Components and Techniques*, K. J. Button, Ed. New York: Academic, 1983, pt. II, vol. 10.
- [22] M. Mojahedi, private communication, 2001.
- [23] K. Agi, K. J. Malloy, E. Schamiloglu, M. Mojahedi, and E. Niver, "Integration of a microstrip patch antenna with a two-dimensional photonic crystal substrate," *Electromagn.*, vol. 19, pp. 277–290, 1999.
- [24] H. Y. D. Yang, N. G. Alexopoulos, and E. Yablonovitch, "Photonic band-gap materials for high-gain printed circuit antennas," *IEEE Trans. Antennas Propagat.*, vol. 45, pp. 185–187, Feb. 1997.
- [25] Y. X. Qian, R. Coccioli, D. Sievenpiper, V. Radisic, E. Yablonovitch, and T. Itoh, "A microstrip patch antenna using novel photonic band-gap structures," *Microwave J.*, vol. 42, p. 66, 1999.
- [26] D. M. Pozar, D. Schaubert, and IEEE Antennas and Propagation Society, *Microstrip Antennas: The Analysis and Design of Microstrip Antennas and Arrays*. New York: IEEE, 1995.
- [27] E. Chang, S. A. Long, and W. F. Richards, "An experimental investigation of electrically thick rectangular microstrip antennas," *IEEE Trans. Antennas Propagat.*, vol. AP-34, pp. 767–772, 1986.
- [28] A. Sabban, "A new broadband stacked two-layer microstrip antenna," in *IEEE Antenna Propagat. Soc. Int. Symp. Dig.*, 1983.
- [29] K. F. Lee, K. Y. Ho, and J. S. Dahele, "Circular-disk microstrip antenna with an air gap," *IEEE Trans. Antennas Propagat.*, vol. AP-32, pp. 880–884, 1984.
- [30] G. Kumar and K. C. Gupta, "Broadband microstrip antennas using coupled resonators," in *IEEE Antenna Propagat. Soc. Int. Symp. Dig.*, 1983.
- [31] R. Coccioli, F. R. Yang, K. P. Ma, and T. Itoh, "Aperture-coupled patch antenna on UC-PBG substrate," *IEEE Trans. Microwave Theory Tech.*, vol. 47, pp. 2123–2130, Sept. 1999.
- [32] D. B. Rutledge and S. E. Schwarz, "Planar multimode detector arrays for infrared and millimeter-wave applications," *IEEE J. Quantum Electron.*, vol. QE-17, pp. 407–414, 1981.
- [33] "The FDTD method as implemented in XFDTD," A Short Course by Remcom Inc., University Park, PA, Mar. 1998.
- [34] C. A. Balanis, *Advanced Engineering Electromagnetics*. New York: Wiley, 1989.
- [35] R. D. Meade, K. D. Brommer, A. M. Rappe, and J. D. Joannopoulos, "Photonic bound-states in periodic dielectric materials," *Phys. Rev. B*, vol. 44, pp. 13 772–13 774, 1991.
- [36] S. L. McCall, P. M. Platzman, R. Dalichaouch, D. Smith, and S. Schultz, "Microwave propagation in 2-dimensional dielectric lattices," *Phys. Rev. Lett.*, vol. 67, pp. 2017–2020, 1991.
- [37] S. John and J. Wang, "Quantum electrodynamics near a photonic band-gap: Photon bound-states and dressed atoms," *Phys. Rev. Lett.*, vol. 64, pp. 2418–2421, 1990.

Kamil Agi (M'98) received the B.S. and M.S. degrees in 1990 and 1992, respectively, from Polytechnic University, Brooklyn, NY, and the Ph.D. degree in 1997 from the University of New Mexico, Albuquerque, all in electrical engineering.

He is currently the President and C.E.O. of K & A Wireless, LLC, Albuquerque, where he guided the development, sales, and marketing of the first digital, spread-spectrum video transmission system for firefighting applications: a key technology in the acceptance of thermal imagers used in firefighting.

Mohammad Mojahedi (M'98), photograph and biography not available at time of publication.

Babar Minhas (S'00), photograph and biography not available at time of publication.

Edl Schamiloglu (F'02) received the B.S. and M.S. degrees from Columbia University, New York, NY, in 1979 and 1981, respectively. He received the Ph.D. degree in applied physics from Cornell University, Ithaca, NY, in 1988.

He is currently Gardner-Zemke Professor in the Electrical and Computer Engineering Department, University of New Mexico, Albuquerque. His research interests include physics and technology of charged particle beam generation and propagation, high-power microwave and ultra-wideband radiation sources, plasma physics and diagnostics, and electromagnetics and wave propagation.

Dr. Schamiloglu is an Associate Editor for the IEEE TRANSACTIONS ON PLASMA SCIENCE, a member of the American Physical Society, a member of the American Society for Engineering Education, and a member of the Cornell Society of Engineers.

Kevin J. Malloy (M'83) received the B.S.E.E. degree from the University of Notre Dame, Notre Dame, IN, in 1978 and the M.S.E.E. and Ph.D. degrees from Stanford University, Stanford, CA, in 1980 and 1984, respectively, all in electrical engineering.

He is currently a member of the Center for High Technology Materials and an Associate Professor with the Electrical and Computer Engineering Department, University of New Mexico, Albuquerque. His research interests include coherent states in semiconductors, disorder in ionic semiconductors, and wave propagation in periodic structures. He is a member of the editorial advisory board for the *CRC Critical Reviews in Solid State and Materials Sciences*.

Dr. Malloy is a member of the IEEE Electron Devices Society, the Materials Research Society, and the American Vacuum Society.